Spin−Orbit Effects, VSEPR Theory, and the Electronic Structures of Heavy and Superheavy Group IVA Hydrides and Group VIIIA Tetrafluorides. A Partial Role Reversal for Elements 114 and 118

Clinton S. Nash*,†

The Glenn T. Seaborg Institute for Transactinium Science, Lawrence Livermore National Laboratory, Livermore, California 94550

Bruce E. Bursten‡

Department of Chemistry, The Ohio State University, 100 West 18th Avenue, Columbus, Ohio 43210

Received: June 23, 1998; In Final Form: September 28, 1998

Relativistic effective core potentials and spin−orbit operators are used in relativistic configuration interaction calculations to explore the effects of spin−orbit coupling on the electronic structures of atoms and molecules of elements 114 and 118. The monohydrides of group IVA and the tetrafluorides of group VIIIA are examined in order to provide examples of trends within families among the various periods. The spin−orbit effect is found to play a dominant role in the determination of atomic and molecular properties. Several nonintuitive consequences of spin−orbit coupling are presented, including the depiction of element 114 as a closed-shell "noble" atom and the suggestion that the VSEPR theory is inadequate to describe the geometry of the rare gas tetrafluoride, $(118)F_4$.

Introduction

Few would argue that as the embodiment of atomic shell structure the periodic table is perhaps the single most powerful tool for the prediction and interpretation of chemical behavior at the chemist's disposal. Its frontier now reaches to the end of the 6d transition series at element 112 and there are reasonable expectations that it will be extended even further.[1] It is appropriate that we should examine the possible chemistry of these superheavy transactinides if for no other reason than to put this venerated tool to the test. This is particularly true given the severe disruptions in periodicity wrought by relativistic effects expected in molecules containing, for instance, atoms of the 7p block ($Z = 113-118$).

That such relativistic effects, net stabilization of s and p shells, net destabilization of d and f shells, and spin−orbit coupling, will be enormous in the superheavy element regime is not really in question. In this contribution, we examine the particular consequences of one of these, spin−orbit coupling, on the chemistry of heavy and superheavy group IVA and group VIIIA atoms in two classes of molecules, monohydrides of the former, SnH, PbH, and (114)H, and tetrafluorides of the latter, XeF_4, RnF_4, and $(118)F_4$. These classes were chosen to illustrate two different but complementary manifestations of the spin−orbit effect in molecules.

In the case of the group IVA monohydrides, the pertinent question concerns the extent to which the fully occupied $7p_{1/2}$ spinor in element 114 resembles a closed atomic shell in the traditional sense and the chemical stablility it therefore confers to the isoated atom vis-à-vis lighter group IVA homologues. As early as the late 1970s, K. Pitzer suggested on the basis of atomic Dirac−Fock calculations that because of spin−orbit effects element 114 would be anomalously inert.[2] It is this proposition that we investigate through simple atomic and molecular calculations.

The second potential manifestation of spin−orbit effects that we examine concerns molecules of the heavier noble gases. Such species have provided pedagogical examples of the usefulness of the valence shell electron pair repulsion (VSEPR) theory, which correctly holds that XeF_4 adopts a square planar geometry about the central Xe atom.[3,4] This is attributed to the presence of six valence electron pairs, two of which are nonbonding, around Xe that minimize their mutual repulsion by adopting an octahedral local arrangement. Electrostatic considerations dictate that the optimal configuration is reached when the unshared pairs lie at 180.0° to one another, and the result is that the four Xe−F bonds describe a square plane with the two lone pairs positioned above and below this plane (Figure 1). Even with the success of VSEPR theory for XeF_4, however, the model is essentially empirical, an a posteriori rationalization for the observed molecular geometry. In treating all of the valence electrons of the noble element as if they were equivalent, interesting questions arise as to its validity for even heavier elements in which differences between the s and p subshells as well as those between spin−orbit components of the p subshell become more pronounced. Such elements include radon and element 118, both of which are group VIIIA atoms. Usual notions about the predictive power of the periodic table and the utility of VSEPR theory would have that both RnF_4 and $(118)F_4$ adopt the same D_{4h} square planar geometry found for XeF_4. This prediction, however, does not take into account these relativistic effects, which are important in Rn and certain to have profound consequences in $(118)F_4$.[5]

Relativistic effects in the geometry of group VIIIA tetrafluorides might manifest themselves in two ways. First, the radial

* Corresponding author.
† E-mail: nash6@llnl.gov.
‡ E-mail: bursten@chemistry.ohio-state.edu.

10.1021/jp982735k CCC: $18.00
Published on Web 01/05/1999

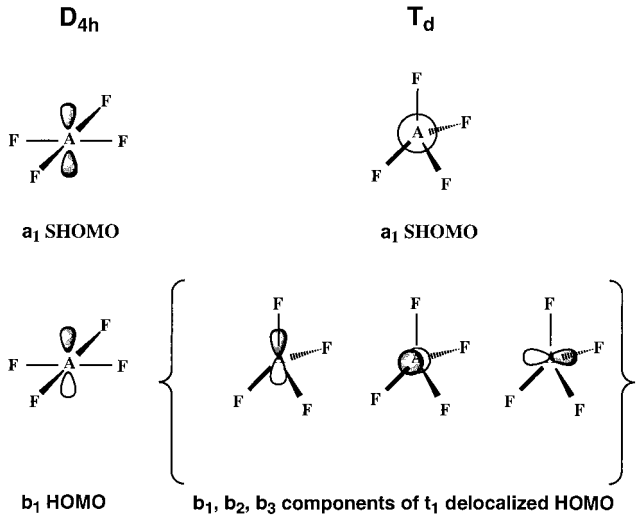

Figure 1. Doubly occupied, nonbonding molecular orbitals of square planar (D_{4h}) and tetrahedral (T_d) noble gas tetrafluorides. The symmetry labels are appropriate for the D_2 subgroup common to both. The depiction of the (delocalized) nonbonding molecular orbitals of tetrahedral noble gas tetrafluorides is not meant to convey the idea that these molecular orbitals are a set of central atom s or p orbitals; they simply have the same symmetry properties.

TABLE 1: Relativistic and Nonrelativistic Dirac−Fock Orbital Eigenvalues (in Hartrees) and Radial Expectation Values (in Bohr) for the Heavy Group VIIIA Elements

	*n*s		*n*p$_{1/2}$		*n*p$_{3/2}$	
	ϵ	$\langle r \rangle$	ϵ	$\langle r \rangle$	ϵ	$\langle r \rangle$
Xe ($n = 5$)						
rel	−1.0102	1.9046	−0.4926	2.2412	−0.4398	2.3516
nonrel	−0.9444	1.9810	−0.4573	2.3380		
rel p (so ave.)			−0.4574	2.3148		
Rn ($n = 6$)						
rel	−1.0727	1.9195	−0.5404	2.2415	−0.3839	2.5826
nonrel	−0.8740	2.1566	−0.4280	2.5434		
rel p (so ave.)			−0.4361	2.4689		
(118) ($n = 7$)						
rel	−1.3322	1.8147	−0.7455	2.0656	−0.3032	2.9776
nonrel	−0.7740	2.4205	−0.3944	2.8203		
rel p (so ave.)			−0.4506	2.6736		

contraction/energetic stabilization of the 6s orbital of Rn or the 7s orbital of element 118 may remove them from the bond-forming valence region and isolate them in some sort of chemically inert outer core. This possibility has already been suggested in the work of Dolg et al., regarding RnF_6.[6] These authors predict that unlike the case of XeF_6, in which the presence of seven valence electron pairs and six bonds about the central atom results in a "psuedo-Jahn−Teller" C_{3v} distortion of the octahedral geometry, the relativistic stabilization of the 6s orbital of Rn effectively removes one electron pair from the valence and thereby favors the higher O_h symmetry. In the case of tetrafluorides, the analogous result would have five valence electron pairs around the central atom and, according to VSEPR theory, a trigonal bipyramidal arrangement of these pairs. The attachment of four ligands would then be expected to result in a disphenoidal (sawhorse) structure of C_{2v} symmetry.

Second, the spin−orbit splitting of the outer p subshell, 6p for Rn and 7p for (118), results in distribution of its electrons into two inequivalent sets, 2 electrons in the *n*p$_{1/2}$ (spinor) orbital and 4 in the *n*p$_{3/2}$ orbital. The results listed in Table 1 clearly illustrate the importance that spin−orbit effects have on the electronic structure of these noble gas atoms, and in particular for element 118.[7] Differences in the eigenvalues and radial expectation values of the p spinors increase dramatically from Xe to (118). In the case of the latter, the data for the 7p$_{1/2}$ spinor are more similar to those of 7s than those of 7p$_{3/2}$. So, inasmuch as the VSEPR model makes distinctions among neither the ns and np electrons nor the spin−orbit components of the p subshell, it remains to be seen how the relativistically augmented inequivalence of these spinors affects results of predictions based on it.

Computational Methods

Shape-consistent relativistic effective core potentials—including spin−orbit operators—and corresponding valence basis sets were used in all of the work reported here.[8] For the transactinide atoms (114) and (118), the 6s, 6p, 6d, 7s, and 7p shells were taken in the valence and the 92 electrons in 1s−5f were replaced by the appropriate RECP. The number of explicitly treated electrons was therefore 22 for element 114 and 26 for element 118. For the lower-period elements of group IVA and group VIIIA, care was taken to ensure that the same numbers of valence electrons were dealt with in each type of calculation, a requirement that naturally leads to a differing core definition for each atom.[9] Despite the fact that common models consider the filled $(n - 1)$s, $(n - 1)$p, and $(n - 1)$d shells to be nonbonding, these "outer core" orbitals were kept in the valence in order to minimize errors resulting from core-valence polarization.[10] For the heavy atoms of both the monohydrides and tetrafluorides, a (6p6sd1f)/[5p5sd1f] basis set contraction pattern was used. In addition, for the RgF_4 calculations the F-1s cores were replaced by the 2-electron RECP of Hurley et al., while the F valence basis sets were taken from Wallace et al. and used under a (4s4p1d)/[2s2p1d] contraction scheme.[11] For the group IVA monohydrides, the hydrogen basis sets were contracted as (4s3p)/[3s2p].

The ECPs were used in relativistic configuration interaction (RCI) calculations using Pitzer's modification of the COLUMBUS quantum chemistry suite.[12,13] The spin−orbit operator was evaluated along with the Coulomb potential at the CI level within the basis of orbitals (atomic or molecular) resulting from spin−orbit averaged, self-consistent field calculations.[14] Configuration lists consisting of occupied and virtual orbitals were spin-adapted in the molecular double point group and used as the MO basis in this relativistic configuration interaction step.[15] The virtual orbitals themselves were improved for correlation using the MVO procedure.[16] This approach facilitates the direct examination of the spin−orbit effect in molecular calculations by alternately allowing the inclusion or exclusion of the spin−orbit operator from the CI Hamiltonian. In such a way the effects of spin−orbit coupling can be distinguished, at least to first order, from those of correlation.

Atoms and Group IVA Monohydrides. All atomic and monohydride calculations were done under D_{2h} and C_{2v} subgroup symmetry, respectively. We have found that as a result of the greater relativistic destabilization/expansion of the "outer-core" 6d shell in 7p-block transactinide atoms relative to the (n − 1)d shell in lighter p-block atoms, the inclusion of 6d excitations can have a surprisingly large impact on calculated atomic excitation energies and ionization potentials.[17] Electron correlation is particularly sensitive to this greater d shell overlap with the outer (s and p) orbitals in the valence region of the atom. To take this into account, we used a variety of active spaces in our calculations on group IVA and VIIIA atoms, ions, and monohydrides that variously included d-doubles, d-singles, and no d excitations. No energy selection schemes were employed, and all one- and two-electron spin−orbit matrix elements within each configuration space were evaluated. For

the monohydrides, practical considerations dictated that in this brute-force approach when doubles from the d shell are included, the reference space be limited to $(n-1)d^{10}ns^2\sigma^2\pi^1$, the minimum that is adequate to describe the electronic structure. A larger reference space would have reduced the size-consistency errors inherent in truncated CI, but because calculated values of R_e and ω_e are less sensitive to these errors, the Langhoff−Davidson correction was applied to only the calculation of the hydride dissociation energies.[18] As this correction is well-defined only for the CID wave function in the absence of a spin−orbit operator, additional (NOSO) calculations were performed excluding single excitations from the configuration lists. The correction to the dissociation energy was taken to be the difference between the size-consistency correction evaluated at the calculated SO−CISD equilibrium bond length and that taken at the limit of the bonding region ($\sim 8.5a_0$). This should therefore be seen as a "correlation-only" size-consistency correction and as such an approximation to an approximation. The approach is justified, however, in recent work by DiLabio et al., who find in their studies of 6p-block monohydrides that individually calculated spin−orbit and correlation effects are nearly additive and can be combined to give highly accurate spectroscopic constants.[19] Finally, a larger reference space including the $(n-1)d^{10}ns^2\sigma^1\pi^2$ configurations but allowing only single $(n-1)$d-excitations was also used to calculate the spectroscopic constants for group IVA monohydrides. We find the agreement between the size-consistency corrected (SCC) and multireference (MR-RCISD) results to be quite satisfactory. A more detailed description of the reference spaces used in the RCI calculations on the atoms and monohydrides is given as Table S1 in the Supporting Information.

Group VIIIA Tetrafluorides. Total RCI energies for XeF_4, RnF_4, and $(118)F_4$ were calculated while varying the central atom−fluorine bond lengths in each of two geometries, square planar (D_{4h}), and tetrahedral (T_d). To explore the particular role that spin−orbit coupling plays in the geometry of these molecules, the bond lengths were also optimized at the CI level excluding the spin−orbit operator. This provides a qualitative illustration of the role of spin−orbit coupling in the determination of the molecular geometry.

For both of the assumed geometries of RgF_4 molecules, the ground state was chosen to be totally symmetric in the double group representation. In the case of D_{4h} molecules this selection is natural and obvious because XeF_4 is known to be a closed-shell molecule. By extension and without consideration of possible relativistic effects, the same might be expected of RnF_4 and $(118)F_4$ in the D_{4h} geometry. While at first glance the choice of this totally symmetric state as the ground state in the tetrahedral cases may seem to be an artificial contrivance, it is not. One can envision a continuous distortion of the square planar structure to the tetrahedral arrangement. In such a distortion the b_1 nonbonding HOMO is delocalized over the entire molecule and becomes degenerate with b_2 and b_3 MOs in a manner similar to a central atom p-orbital in a tetrahedral field. Meanwhile, the nonbonding a_1 SHOMO (second-highest molecular orbital) also becomes delocalized in a manner analogous to a central atom s orbital. These molecular orbital "mappings" are illustrated in Figure 1 (T_d). The result is the generation of an open-shelled "p^2" molecular orbital configuration that relies on an appropriate spin-coupling to recover the totally symmetric state. Inasmuch as the case of an inert $7p_{1/2}$ closed-shell spinor and the occurrence of bonding interactions through the $7p_{3/2}$ spinor constitutes such a spin-coupling, the choice is in keeping with the model being tested. In fact, in test calculations on tetrahedral $(118)F_4$ at the equilibrium bond length, it was found that the lowest excited, multiply degenerate state corresponding to this open-shell (AREP) MO configuration lies at least 5.6 eV above the totally symmetric ground state.

The active space in the spin−orbit configuration interaction calculations for all RgF_4 molecules in both geometries consisted of single excitations of 24 electrons in 12 doubly occupied molecular orbitals into 14 virtual orbitals. Double excitations were allowed from the molecular orbital that corresponds to the b_1 HOMO in the square planar geometry and to the degenerate '$p^2/(b_1, b_2, b_3)^2$" delocalized MO in the tetrahedral geometry. The only additional net doubles that were allowed consisted of single excitations from the HOMO in conjunction with singles from the set of 12 active orbitals mentioned earlier. The CI space that resulted from this prescription consisted of 4824 and 12 336 double group functions for the D_{4h} and T_d structures, respectively.

The AREP-SCF description of the T_d molecule requires a multideterminential wave function apart from any involvement of spin−orbit coupling. This demands the use of six different reference configurations in order to generate a configuration list roughly equivalent to the single one used in the D_{4h} geometry. Therefore, to obtain configuration lists of manageable size when spin−orbit coupling is included, this somewhat restricted active space definition was adopted. As the majority of the spin−orbit effect is captured at the CI-singles level, however, it is believed that the quality of the calculations for RgF_4 molecules are on the order of that of the Dirac−Fock method, or perhaps somewhat higher as some degree of dynamic correlation is included.[19]

Finally, the geometry of $(118)F_4$ was also optimized at the SCF level in the absence of spin−orbit coupling under the constraints of C_{2v} symmetry using the GAMESS quantum chemistry package.[20] The choice of C_{2v} as the "computational" symmetry was made because, as a subgroup common to all of the considered geometries (T_d, D_{4h}, and C_{2v}-sawhorse), all are sampled in the optimization and the location of the potential energy minimum was able to proceed without undue prejudice.

Results and Discussion

Atoms. The electrons of neutral element 114 fill the $7p_{1/2}$ spinor orbital giving a $J = 0$, $7s^27p_{1/2}^2$ ground state. The energetic separation of this "closed shell" state from the lowest, $J = 1$, $7s^27p_{1/2}^17p_{3/2}^1$ "open-shell" state is variously calculated as 3.679 eV using RCI with d-doubles (RCI-dd), 3.851 eV with d-singles (RCI-d), and 3.960 eV allowing no d excitations (RCI-nod). The $J = 2$ electronic coupling from the open $7s^27p_{1/2}^17p_{3/2}^1$ configuration lies 4.166 eV (RCI-dd) above the ground state and the doubly excited $J = 2$ $7s^27p_{3/2}^2$ state lies 8.512 eV (RCI-dd) above the ground state. These excitation energies indicate a strong tendency for the $7p_{1/2}$ spinor orbital to remain a closed shell. In addition, the element 114 first ionization potential of 8.510 eV (RCI-dd) is only marginally lower in energy than the excitation energy to the second $J = 2$ state, which, from a nonrelativistic standpoint, is simply a higher multiplet term of the same (LS) electron configuration. The corresponding calculated excitations for Pb occur at energies roughly one-quarter of those in (114) and the excitations for Sn a smaller fraction of these. Table 3 compares the atomic excitation energies of Sn, Pb, and element 114. These results indicate the clear tendency for a dramatic increase in the stability of closed spinor shells from Sn to element 114 with by far the more drastic step being that from Pb to element 114. Calculations performed at all allowed levels of 6d-shell excitation also indicate the first

TABLE 2: Electronic Excitation Energies and Ionization Potentials of Elements 114 and 118 and Their Ions Calculated Using the Relativistic Configuration Interaction Methods with d-Doubles (RCI-dd), d-Singles (RCI-d), and No d (RCI-nod) Excitations Allowed[a]

atom	J (parity)	ΔE ($E - E_0$) (eV) RCI-dd	RCI-d	RCI-nod	primary configuration (under jj coupling)
(114)					
	0 (+)	0.0	0.0	0.0	$7s^27p^{*2}$
	1 (+)	3.679	3.851	3.960	$7s^27p^{*1}7p^1$
	2 (+)	4.166	4.312	4.337	$7s^27p^{*1}7p^1$
	2 (+)	8.512	9.025	9.348	$7s^27p^2$
IP		8.510	8.842	8.886	$7s^27p^{*2} \rightarrow$
IP(SCC)		8.564	8.882	8.897	$7s^27p^{*1} + e^-$
$(114)^+$					
	1/2 (−)	0.0	0.0	0.0	$7s^27p^{*1}$
	3/2 (−)	5.433	5.748	5.930	$7s^27p^1$
(118)					
	0 (+)		0.0	0.0	$7s^27p^{*2}7p^4$
	2 (−)		3.631	3.884	$7s^27p^{*2}7p^38s^1$
	1 (−)		4.329	4.590	$7s^27p^{*2}7p^38s^1$
	0 (−)		13.046	12.206	$7s^27p^{*1}7p^48s^1$
	1 (−)		13.433	10.911	$7s^27p^{*1}7p^48s^1$
IP		7.210	7.372	7.616	$7s^27p^{*2}7p^4 \rightarrow$
IP(SCC)		7.318	7.460	7.667	$7s^27p^{*2}7p^3 + e^-$
$(118)^+$					
	3/2 (−)	0.0	0.0	0.0	$7s^27p^{*2}7p^3$
	1/2 (−)	11.401	11.695	10.098	$7s^27p^{*1}7p^4$

[a] The ionization potentials are corrected for extensivity using the Langhoff-Davidson correction.

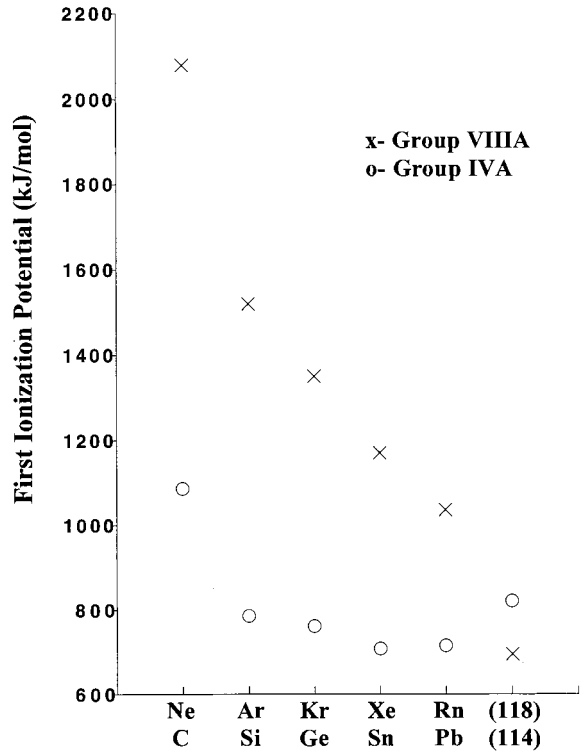

Figure 2. Comparisons of the first ionization potentials of group IVA and group VIIIA atoms. The values for C−Pb and Ne−Rn are experimental (ref 22) while those for element 114 and element 118 are from RCI-dd calculations.

ionization potential of element 114 to be higher than that of element 118. This inversion of the usual ordering is depicted in Figure 2, a plot of the first IPs of the carbon family of elements and the noble gases.[21]

The enormous inequivalence of the spin−orbit components of the p subshell in element 118 is illustrated in its cation, $(118)^+$, which is calculated to have a $^2P_{3/2}-{}^2P_{1/2}$ splitting of 11.401 eV. Although this interval is certainly exaggerated by the fact that this is a +1 ion, we also see from the results in Table 2 that there is a large energy gap, ∼9 eV, between states resulting from $7p_{3/2} \rightarrow 8s$ electron transitions and those resulting from $7p_{1/2} \rightarrow 8s$ transitions in the neutral atom. The corresponding experimentally determined gaps in Xe and Rn are ∼1 and ∼4 eV, respectively.[22] This energy difference surpasses the calculated (RCI-dd) ionization potential of 7.210 eV (RCI-dd) and implies that it is easier to ionize the atom than it is to promote an electron from the lower spin−orbit component of the 7p orbital to the already relativistically stabilized 8s orbital. At the same time, we find that these $7p_{3/2} \rightarrow 8s$ transitions occur at energies roughly 55−56% of those for the analogous excitations in Rn while the $7p_{1/2} \rightarrow 8s$ transitions are 120−130% higher.[22] These results illustrate the enhanced importance of both the "extravalent" s-shell and valence $p_{1/2}$ shell stabilization in (118) relative to Rn and suggest that they will have important chemical consequences.

These atomic results are symptomatic of a reorganization in the shell structure of p-block transactinides, in which the salient feature is the closing of the $7p_{1/2}$ spinor orbital, which is perhaps more reminiscent of an atomic shell closing than the completion of the 7p-block as a whole at element 118. Just how change in the atomic nature of the atoms might affect their possible chemistry is the subject of the next section.

TABLE 3: Lowest Electronic Excitations and Ionization Potentials of the Heavy Group IVA Atoms Pb and Sn and Their Ions[a]

state J (parity)	ΔE ($E - E_0$) (eV) RCI-dd	RCI-d	RCI-nod	expt[21]	primary configuration (under jj coupling)
Pb					
0 (+)	0.0	0.0	0.0	0.0	$6s^26p^{*2}$
1 (+)	0.851	0.871	0.869	0.969	$6s^26p^{*1}6p^1$
2 (+)	1.293	1.315	1.302	1.320	$6s^26p^{*1}6p^1$
2 (+)	2.611	2.666	2.638	2.660	$6s^26p^2$
0 (+)			3.749	3.653	$6s^26p^2$
IP	7.005	7.088	7.036	7.415	$6s^26p^{*2} \rightarrow$
IP(SCC)	7.042	7.112	7.048		$6s^26p^{*1} + e^-$
Pb^+					
1/2 (−)	0.0	0.0	0.0	0.0	$6s^26p^{*1}$
3/2 (−)	1.631	1.678	1.664	1.746	$6s^26p^1$
Sn					
0 (+)	0.0	0.0	0.0	0.0	$5s^25p^{*2}$
1 (+)	0.180	0.181	0.176	0.210	$5s^25p^{*1}5p^1$
2 (+)	0.396	0.399	0.387	0.425	$5s^25p^{*1}5p^1$
2 (+)	1.247	1.236	1.207	1.068	$5s^25p^2$
0 (+)			2.283	2.128	$5s^25p^2$
IP	7.144	7.093	7.049	7.342	$5s^25p^{*2} \rightarrow$
IP(SCC)	7.180	7.115	7.065		$5s^25p^{*1} + e^-$
Sn^+					
1/2 (−)	0.0	0.0	0.0	0.0	$5s^25p^{*1}$
3/2 (−)	0.455	0.488	0.485	0.577	$5s^25p^1$
Rn					
IP	10.096	10.146	10.181	10.746	
IP(SCC)	10.209	10.234	10.243		
Rn^+					
3/2 (−)	0.0	0.0	0.0	0.0	$6s^26p^{*2}6p^3$
1/2 (−)	3.675	3.697	3.722	3.831	$6s^26p^{*1}6p^4$
Xe					
IP	11.601	11.645	11.635	12.127	
IP(SCC)	11.718	11.745	11.715		
Xe^+					
3/2 (−)	0.0	0.0	0.0	0.0	$5s^25p^{*2}5p^3$
1/2 (−)	1.232	1.230	1.220	1.307	$5s^25p^{*1}5p^4$

[a] The comperable data for (114) are listed in Table 1. The ionization potentials are corrected for extensivity using the Langhoff−Davidson correction.

TABLE 4: Spectroscopic Constants of Group IVA Monohydrides Calculated at the Relativistic Configuration Interaction Level with Varying Degrees of Allowed d Excitations[a]

molecule	state	R_e (Å)	ω_e (cm^{-1})	D_e (eV)
(114)H				
RCISD nod	$\Omega = 1/2$	2.064	977	0.54
RCISD d singles	$\Omega = 1/2$	1.977	1164	0.79
RCISD d singles + ΔE(SCC)				0.49
RCISD d singles (NOSO)	$^2\Pi$	1.947	1528	>2.86
MR-RCISD d singles	$^2\Pi$	1.993	1079	0.62
RCISD d doubles	$\Omega = 1/2$	1.954	1222	0.90
RCISD d doubles + ΔE(SCC)				0.59
(HgH) expt[23]	$^2\Sigma^+$	1.766	1203	0.524
$(114)H^+$				
RCISD d singles	$\Omega = 0^+$	1.736	1702	2.88
PbH				
RCISD nod	$\Omega = 1/2$	1.883	1502	1.88
RCISD d singles	$\Omega = 1/2$	1.890	1546	2.12
RCISD d singles + ΔE(SCC)				1.69
RCISD d singles (NOSO)	$^2\Pi$	1.888	1576	>2.80
MR-RCISD d singles	$\Omega = 1/2$	1.890	1541	1.81
expt[23]		1.839	1564	≤1.686
SnH				
RCISD nod	$\Omega = 1/2$	1.831	1607	2.69
RCISD d singles	$\Omega = 1/2$	1.825	1619	2.80
RCISD d singles + ΔE(SCC)				2.40
RCISD d singles (NOSO)	$^2\Pi$	1.825	1617	2.97
MR-RCISD d singles	$\Omega = 1/2$	1.825	1614	2.59
expt[23,28]		1.781	1718	2.43

$$\Delta E(\mathrm{SCC}) = \Delta E_{\mathrm{CID}}(r = R_e, \mathrm{NOSO}) - \Delta E_{\mathrm{CID}}(r = 8.5\ a_0, \mathrm{NOSO})$$
$$\Delta E = (1 - \sum C_0^2) E_{\mathrm{corr}}.$$

[a] NOSO indicates that the calculation was performed in the absence of a spin−orbit potential. The data for HgH are included for comparison.

SnH, PbH, and (114)H

The $\Omega = 1/2$ ground-state potential energy surface of (114)H in Figure 3 exhibits a shallow minimum with a well depth of less than 0.04 Hartrees. This state corresponds to the interaction of a hydrogen atom with the $J = 0(+)$ ground state of element 114, and the result is something more than a van der Waals complex but certainly falls short of a full bond. Because of the enormous energetic separation of the spinor components of the 7p shell in element 114, there is relatively little of the participation in bonding of the $\omega = 1/2$ projection of the $7p_{3/2}$ atomic spinor that is necessary for the formation of a full σ bond. More importantly, as a closed, stable, atomic shell, the $7p_{1/2}$ spinor orbital resists participation in the formation of hybrid states with open-shell (spinor) configurations more suitable for bonding. The fact that there is any bonding at all is an indication that some higher atomic states of element 114 do mix with the ground state and allow a slight relaxation of the closed spinor in the molecular field, but clearly this occurs only to a limited extent.

The next two states are well separated from the ground state and represent the interaction of the hydrogen atom with the open $7s^27p_{1/2}^17p_{3/2}^1$-excited-state configuration of element 114. The gap between the ground and excited potential energy surfaces at the dissociated atom limit corresponds to the difference between the closed $J = 0$ $(7p_{1/2}^2)$ and $(J = 1)$ $7p_{1/2}^17p_{3/2}^1$ atomic states. The dissociation energies for the excited states are at least double that of the ground state, and their widely separated potential minima roughly depict the interaction of the hydrogen with each of the two singly occupied and radially dissimilar 7p-spinor orbitals.

It is apparent from Figure 3 that the inclusion of double excitations from the set of d orbitals makes only a small

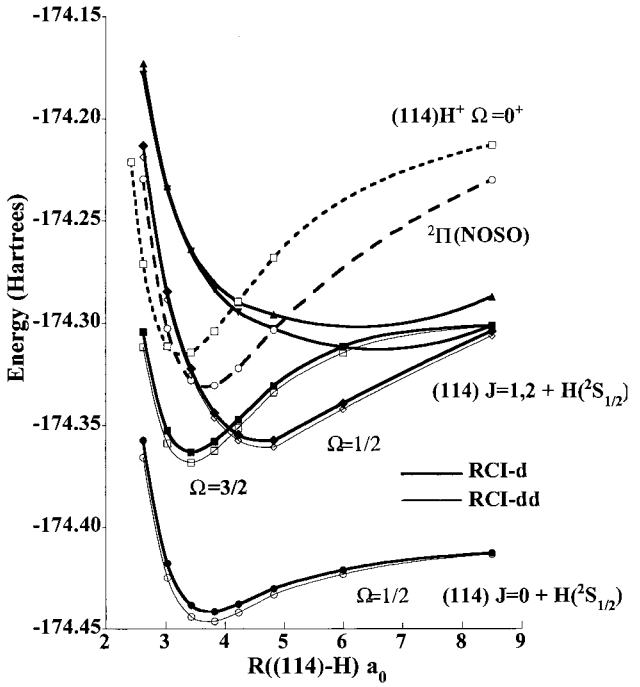

Figure 3. Potential energy surface of the $\Omega = 1/2$ ground and $\Omega = 3/2$, $1/2$ lowest excited states of (114)H compared to the $(^2\Pi)$ $\Lambda = 1$ ground state in the molecule in the absence of spin−orbit coupling and the $\Omega = 0^+$ ground cationic state. For the molecular spin−orbit states, the lower components of the doubled curves correspond to the PES calculated with d-double excitations.

difference in the overall depth or shape of the various potential energy surfaces. This contrasts to the case for (113)H ($\Omega = 0^+$, $7s^27p\sigma^2$) in which d-doubles have been found to be quite important.[17] Evidently, the overlap, and hence correlation, of the 6d shell with the molecular valence orbitals has diminished sufficiently that, by element 114, it is only marginally important to the chemistry of the element, at least in this low oxidation state. However, there is a more significant difference in the well depth when 6d excitations are excluded entirely from the configuration list. It seems that spin−orbit contributions resulting from at least the 6d-singles should be included in the theoretical treatment of element 114 and its molecules.

The chemical inertness suggested in the atomic results is therefore supported in the results of these molecular calculations, at least for this σ-dominant interaction. While the ground state potential energy surface is not purely repulsive as it is in, for example, a noble gas complex such as NeH or ArH, one might expect that at all but very low temperatures atom−atom scattering or vibrational predissociation would dominate over any bond formation in such a species. That this is a combined result of both the spin−orbit effect and the double occupancy of the $7p_{1/2}$ spinor of element 114 is evidenced by the return of a substantial bonding interaction with either the nullification of the spin−orbit potential to produce a true $^2\Pi$ molecular ground state or the loss of an electron to allow the interaction of hydrogen with the open-shelled cation, $(114)^+$. The case of closed-shell element 114 and its relative chemical inactivity is an extreme example of trends seen in earlier periods.

Figures 4 and 5 are analogous potential energy curves for PbH and SnH. In the latter, the spin−orbit effect is seen to induce a slight splitting of the $^2\Pi$ term that is small compared to the overall calculated well depth of about 2.59 eV(MR-RCISD). The $\Lambda-\Sigma$ parentage of the ground and first excited states of SnH is clearly discernible in contrast to the case in (114)H, where it is not. In PbH, the splitting is noticeably greater

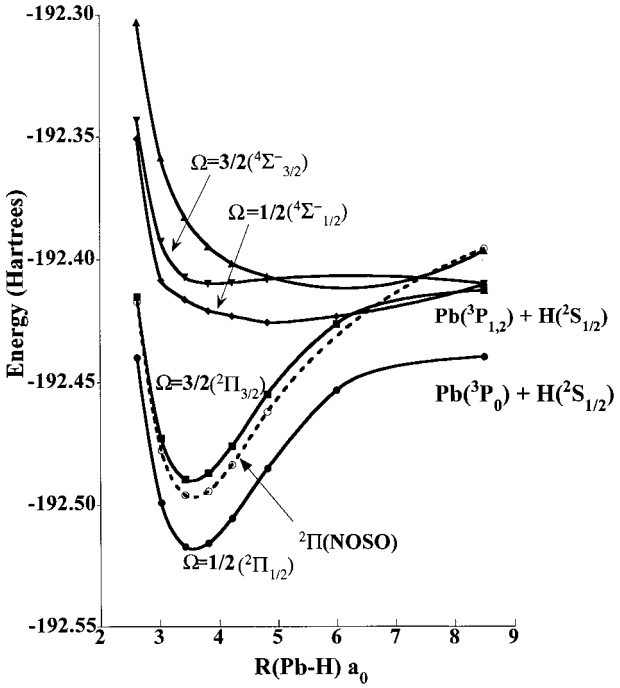

Figure 4. Potential energy surface of the five lowest states of PbH. The dashed curve is for the ($^2\Pi$) $\Lambda = 1$ ground state in the absence of spin−orbit coupling. The calculations were performed at the RCI-d level.

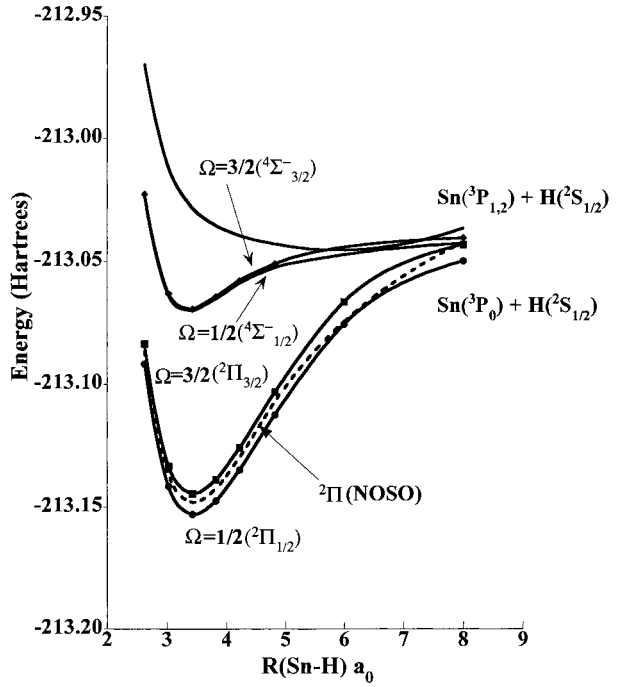

Figure 5. Potential energy surface of the five lowest states of SnH. The dashed curve is for the ($^2\Pi$) $\Lambda = 1$ground state in the absence of spin−orbit coupling. The calculations were performed at the RCI-d level.

than in SnH but is still smaller than the overall bonding interaction calculated at approximately 1.81 eV. These compare to the analogously calculated dissociation energy of 0.62 eV for (114)H. Although the dissociated atom limits again are different for the ground and excited states of both PbH and SnH, the gaps between the respective potential energy surfaces at $R \rightarrow \infty$ are smaller than in (114)H, befitting the more modest spin−orbit effects expected for these atoms. When the equilibrium dissociation energies were corrected for size-consistency using the Langhoff−Davidson formula, very good agreement with available experimental values for PbH and SnH was obtained. This lends weight to the prediction that (114)H would have a very weak bond compared to PbH and SnH with a SC-corrected dissociation energy on the order of 0.5−0.6 eV. By comparison, this equilibrium hydride dissociation energy is roughly equal to that of the "noble metal" Hg, determined to be 0.524 eV.[23] A more complete treatment of size-consistency in the evaluation of the spin−orbit operator, for instance by using Kramers' restricted coupled-cluster technique, might find the (114)H D_e to be lower still. Nevertheless, because the majority of the spin−orbit effect is captured at the CI-singles level and because single excitations at least from all important references are present in the configuration list, the size-consistency errors stemming from the evaluation of the spin−orbit operator should be relatively small. In the absense of experimental evidence for (114)H, or the even the near-term prospect of obtaining any, it sufficies to say that element 114 would probably be at least as chemically stable as mercury.

XeF_4, RnF_4, and $(118)F_4$

Using GAMESS, the SCF geometry optimization of $(118)F_4$ (without spin−orbit coupling) converged to a square planar arrangement with a (118)-F bond length of 2.124 Å. The limitation to C_{2v} not only allowed the sawhorse configuration to be sampled in the optimization procedure but in fact it was chosen as the starting structure. Still, the convergence to the D_{4h} geometry in the SCF optimization with inclusion of scalar relativistic but not spin−orbit effects demonstrates that the stabilization of the 7s shell does not in itself remove it from the valence. That the 7s orbital is not made stereochemically inactive by scalar relativistic effects in $(118)F_4$ is a result in accord with its periodic analogy to XeF_4. As this was found to be the case for $(118)F_4$, no comparable calculation for Rn or Xe was performed.

The RCI results for these noble element tetrafluorides are somewhat different. As seen in Figure 6, the total energy of XeF_4 in the D_{4h} configuration as a function of Xe−F bond length is well below that of the tetrahedral geometry. This is true both with and without the inclusion of spin−orbit coupling, which is found to have a negligible impact. The calculated equilibrium Xe−F distance of 1.95 Å is in good agreement with the experimental value of 1.935 Å.[24] The relative unimportance of spin−orbit coupling in the geometry of xenon tetrafluoride is a measure of the validity of the Russell−Saunders (LS) coupling scheme for this molecule.

As shown in Figure 7, the calculated results for RnF_4 are qualitatively very similar to those of XeF_4 with the T_d configuration lying at least 2.7 eV above the D_{4h} potential energy surface at the latter's equilibrium bond length. This Rn−F bond length is calculated at around 2.05 Å compared to 2.025 Å in a similar ECP calculation by Dolg et al.[25] Currently, experimental data are not available for RnF_4. Again, we see that over the range of bond lengths examined, the tetrahedral potential energy curve shows no sign of reaching a minimum and the situation is only exacerbated in the spin−orbit-less calculation. The increased importance of spin−orbit coupling in radon tetrafluoride over the xenon compound is evident, however, with the D_{4h} PES calculated in the absence of spin−orbit effects being noticeably higher in energy than that in the fully relativistic case. This is indicative of the beginning of a breakdown in the Russell−Saunders coupling scheme in molecules containing heavy atoms. If prepared, RnF_4 would be expected to adopt a square planar D_{4h} configuration in accord with its placement in the periodic table, substantial spin−orbit effects notwithstanding.

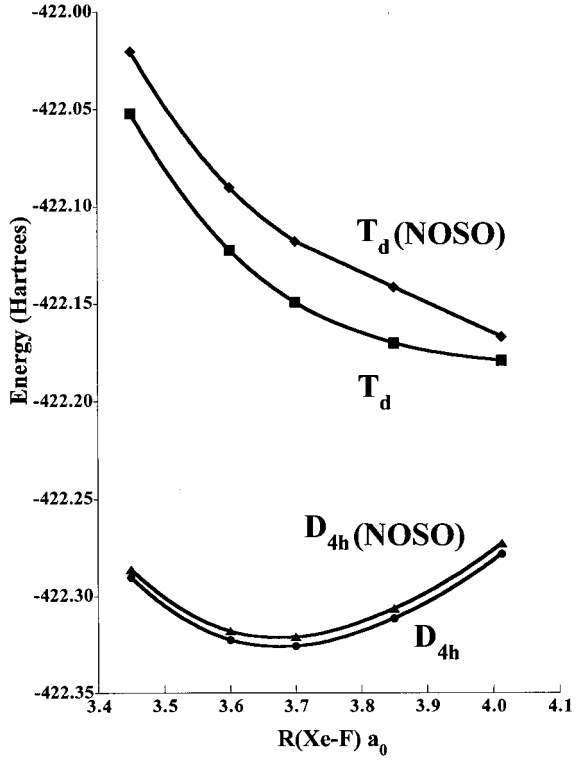

Figure 6. Variation in total energy of XeF_4 with bond length in two different geometries, tetrahedral (T_d) and square planar (D_{4h}), with and without spin−orbit coupling.

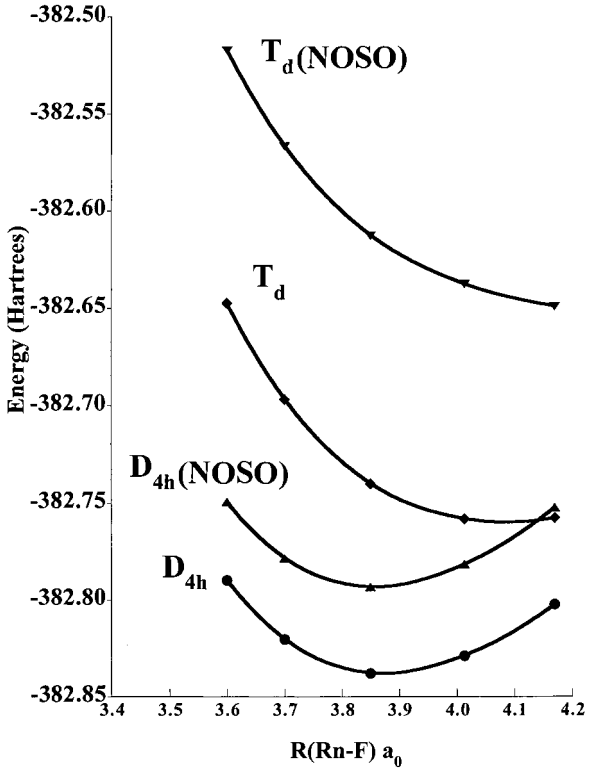

Figure 7. Variation in total energy of RnF_4 with bond length in two different geometries, tetrahedral (T_d) and square planar (D_{4h}), with and without spin−orbit coupling.

The situation as depicted in Figure 8 for $(118)F_4$ is fundamentally different. In the absence of spin−orbit coupling, the VSEPR-consistent results again hold with the D_{4h} structure being markedly lower in energy and having an equilibrium bond length of 2.127 Å−very similar to the previously mentioned (GAMESS)

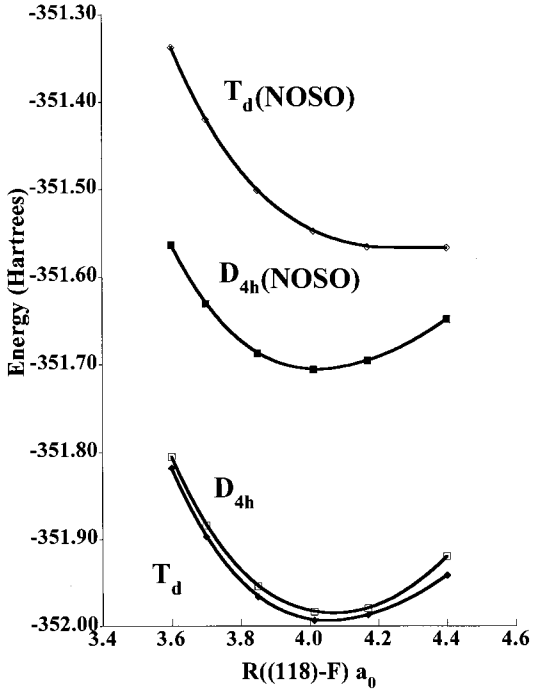

Figure 8. Variation in total energy of $(118)F_4$ with bond length in two different geometries, tetrahedral (T_d) and square planar (D_{4h}), with and without spin−orbit coupling.

SCF-optimized bond length. And, again, the PES of spin−orbitless T_d structure is mostly dissociative. When spin−orbit coupling is included, however, not only does the potential energy surface of the tetrahedral structure become competitive with that of the D_{4h} geometry, it actually falls slightly (∼0.25 eV) below it. On the basis of these results, one would conclude that if it were prepared, the tetrafluoride of element 118 would be tetrahedral with a (118)−F bond length of around 2.14 Å. At the very least, $(118)F_4$ would have to be considered stereochemically nonrigid.

At this level of calculation, the difference in energy between the two geometries of $(118)F_4$ is still fairly small and it could well be that an improved treatment of correlation will bring the D_{4h} surface below that of the T_d structure. On the other hand, the active molecular orbitals for T_d $(118)F_4$ were generated in a somewhat ad hoc manner, and it is certainly true that they are less appropriate for a CI study than are the MOs under the D_{4h} geometry. It could therefore just as easily be the case that a more complete multiconfigurational treatment with extensive dynamic as well as nondynamic correlation will lower the energy of the T_d relative to the D_{4h} structure to an even greater extent. Such a treatment would more fully incorporate contributions from the 8s orbital and $8p_{1/2}$ spinor into the bonding scheme, which would improve the description of hybridization about the central atom.

The real surprise is that the potential energy surfaces are at all competitive; this flies in the face of predictions based on a simplistic interpretation of the periodic table. It is, however, quite understandable in terms of what we have already discussed about spin−orbit coupling in these atoms. The result of the enormous spin−orbit splitting of the 7p shell of element 118 is the generation of an inert pair of $7p_{1/2}$ electrons in addition to the inert pair in the 7s orbital. The net effect is to remove two electron pairs from the valence and produce an atom that must be considered essentially tetravalent.

It is perhaps curious that the D_{4h} geometry was preferred in the GAMESS SCF optimization. If the 7s electrons are thought

of as an inert pair in the discussion of the spin−orbit CI results, then why did they not behave as such in the SCF results where spin−orbit effects are neglected? This apparent inconsistency is resolved if one considers that the spin−orbit averaged 7p shell is a poor representation of the element 118 valence p electrons. From Dirac−Fock results of Table 1 it is seen that there is a 0.91 a_0 difference in the radial expectation values and a 0.44 Hartree difference in the eigenvalues of the 7p spin−orbit components. The $7p_{1/2}$ spinor is more similar in energy and radial behavior to the 7s orbital than to its own spin−orbit counterpart. In the spin−orbit averaged case, the valence of the atom is dominated by six equivalent 7p electrons. The 7s orbitals are still reasonably close in energy to them and probably not well shielded from chemical interactions by them. When spin−orbit effects are included, however, the 7s orbitals are shielded from the valence by the very stable, spherical $7p_{1/2}$ spinor. In turn, the $7p_{3/2}$ electrons are more effectively shielded from the nuclear charge and are therefore more polarizable.

This proposition was tested with an additional spin−orbit configuration interaction calculation of the $(118)F_4$ in the "sawhorse" geometry at the equilibrium (T_d) (118)−F bond length. It was found that this structure was higher in energy than both the T_d and D_{4h} configurations when spin−orbit coupling was allowed. Interestingly, without the spin−orbit operator in the CI Hamiltonian, this configuration was found to be lower in energy than the tetrahedral geometry but still higher than the D_{4h} geometry. These findings seem to support the idea that the inner 7s electrons are shielded from the valence and joined by the $7p_{1/2}$ electrons in a kind of outer core.

Conclusions

These results indicate that relativistic shell and spin−orbit effects cooperate to change the valency of both (114) and (118) relative to other members of their chemical groups. In several respects, element 114 behaves like a noble gas with a characteristically high first ionization potential and resistance to bond formation. At the same time, element 118 is more like a carbon group element with a lower first ionization potential and enhanced tendency to adopt a tetrahedral local environment. These results indicate that there is at least a partial role reversal of these two elements wherein the filling of the $7p_{1/2}$ spinor shell is at least if not more chemically relevant than the filling of the entire 7p shell. In any case, the tetravalency of element 118 is not seen in earlier periods wherein the tetrafluorides of xenon and radon conform to the precepts of the VSEPR theory. Nor is the indifferent interaction of element 114 and hydrogen suggested by the behavior of lower-period carbon group elements. Seth et al. come to similar conclusions in recent work comparing the stability, or rather instability, of the +4 oxidation state of element 114 with those of other Group IVA atoms.[26]

Although exceptions to the VSEPR model are not unknown, they most frequently occur in transition metal compounds and involve nonspherical distortions of the metallic outer core.[27] They are understood to be the result of complicated electrostatic and covalent interactions and the theory can be adjusted to account for them. The fact that we have found a possible exception in the main group should give pause to anyone who would apply the model uncritically. Modern VSEPR theories are based on the analysis of electron density domains and its Laplacian and in this respect have been put on a firm theoretical foundation.[28] Our studies indicate, however, that one neglects spin−orbit effects in valence theories at some peril, especially for heavy elements. To be sure elements 114 and 118 represent extreme examples of this, ones that are not likely to be encountered in practice. Still, it is by examining extreme cases that we become familiar with principles that may be applicable to more typical problems.

Acknowledgment. The authors thank Dr. R. M. Pitzer and Dr. W. C. Ermler for their assistance at various stages of this work. Thanks also to the Ohio Supercomputer Center and the National Energy Research Supercomputer Center for generous grants of computer time and to Dr. D. C. Hoffman for her support in this effort. B.E.B. gratefully acknowledges support for this research from the Division of Chemical Sciences, U.S. Department of Energy (Grant DE-FG02-86ER 13529). Finally, thanks to Dr. P. Schwerdtfeger and Dr. M. Seth for their helpful comments.

Supporting Information Available: Table S1, which describes in greater detail the active and reference spaces used in the atomic and group IVA monohydride calculations, and Table S2, which contains the RECP and basis set data used for Sn, Pb, Xe, and Rn (7 pages). Ordering information is given on any current masthead page.

References and Notes

(1) Hoffman, D. C. In *Actinides and the Environment*; Sterne, P. A., et al (eds), 3−22 1998.

(2) Pitzer, K. *J. Chem. Phys*. **1975**, 63, 1032.

(3) Hyman, H. H. *Noble-Gas Compounds*; University of Chicago Press: Chicago, 1963.

(4) Classen, H. H.; Selig, H.; Malm, J. G. *J. Am. Chem. Soc*. **1962**, *84*, 3593.

(5) (a) Ishikawa, Y.; Koc, K. *Phys. Rev. A* **1994**, *50*, 4733. (b) Kim, M. C.; Lee, S. Y.; Lee, Y. S. *Chem. Phys. Lett*. **1996**, *253*, 216. (c) Küchle, W.; Dolg, M.; Stoll, H.; Preuss, H. *Mol. Phys*. **1991**, *74*, 1245.

(6) Dolg, M.; Küchle, W.; Stoll, H.; Preuss, H.; Schwerdtfeger, P. *Mol. Phys*. **1991**, *74*, 1265.

(7) Desclaux, J. P. *At. Data Nucl. Data Tables* **1973**, *12*, 311.

(8) Nash, C. S.; Bursten, B. E.; Ermler, W. C. *J. Chem Phys*. **1997**, *106*, 5133.

(9) 22 valence electron ECPs and basis sets for Sn and Pb as well as 26 valence electron ECPs and basis sets for Xe and Rn are from unpublished results. They are included in Supporting Information as Table S2.

(10) Schwerdtfeger, P.; Szentpaly, L.; Vogel, K.; Silberbach, H.; Stoll, H.; Pruess, H. *J. Chem. Phys*. **1986**, *84*, 1606.

(11) (a) Hurley, M. M.; Pacios, L. F.; Christiansen, P. A.; Ross, R. B.; Ermler, W. C. *J. Chem. Phys*. **1986**, *87*, 2812. (b) Wallace, N. M.; Blaudeau, J. P.; Pitzer, R. M. *Int. J. Quantum Chem*. **1991**, *40*, 789.

(12) Shepard, R.; Shavitt, I.; Pitzer, R. M.; Comeau, D. C.; Pepper, M.; Lischka, H.; Szalay, P. G.; Ahlrichs, R.; Brown, F. B.; Zhao, J. G. *Int. J. Quantum Chem. Symp*. **1989**, *22*, 149.

(13) Ermler, W. C.; Ross, R. B.; Christiansen, P. A. *Adv. Quantum Chem*. **1988**, *19*, 139.

(14) (a) Chang, A.; Pitzer, R. M. *J. Am. Chem. Soc*. **1989**, *111*, 2500. (b) Chang, A.; Pitzer, R. M. programs: ARGOS, CNVRT, SCFPQ, LSTRN, CIDBG.

(15) (a) Pitzer, R. M.; Winter, N. W. *J. Phys. Chem*. **1988**, *92*, 3061. (b) Pitzer, R. M.; Winter, N. W. *Int. J. Quantum Chem*. **1991**, *40*, 773.

(16) Bauschlicher, C. W., Jr. *J. Chem. Phys*. **1980**, *72*, 880.

(17) Nash, C. S.; Bursten, B. E. Unpublished manuscript.

(18) Langhoff, S. R.; Davidson, E. R. *Int. J. Quantum Chem*. **1974**, *8*, 61.

(19) DiLabio, G. A.; Christiansen, P. A. *J. Chem. Phys*. **1998**, *108*, 7527.

(20) Schmidt, M. W.; Baldridge, K. K.; Boatz, J. A.; Elbert, S. T.; Gordon, M. S.; Jensen, J. H.; Koseki, S.; Matsunaga, N.; Nguyen, K. A.; Su, S.; Windus, T. L.; Dupuis, M.; Montgomery, J. A. *J. Comput. Chem*. **1993**, *14*, 1347.

(21) Huheey, J. E.; Keiter, E. A.; Keiter, R. L. *Inorganic Chemistry Principles of Structure and Reactivity*, 4th ed.; Harper Collins: New York, 1993.

(22) Moore, C. E. *Atomic Energy Levels;* Circular of the National Bureau of Standards 467; U.S. Government Printing Office: Washington, DC, 1958; No. 3, p 228.

(23) Huber, H. P.; Herzberg, G. *Constants of Diatomic Molecules*; Molecular Spectra and Molecular Structure; Van Nostrand Reinhold: New York, 1979; Vol. 4.

(24) (a) Bürger, H.; Ma, S.; Breidung, J.; Thiel, W. *J. Chem. Phys*. **1996**, *104*, 4945. (b) Styszynski, J.; Malli, G. *Int. J. Quantum Chem*. **1995**, *55*, 227. (c) Styszynski, J.; Cao, X.; Malli, G. L.; Visscher, L. *J. Comput. Chem*. **1997**, *18*, 601.

(25) Dolg, M.; Küchle, W.; Stoll, H.; Preuss, H.; Schwerdtfeger, P. *Mol. Phys*. **1991**, *74*, 1265.

(26) Seth, M.; Faegri, K.; Schwerdtfeger, P. *Angew. Chem., Int. Ed. Engl*. **1998**, *37*, 2493.

(27) Gillespie, R. J.; Bytheway, I.; Tang, T. H.; Bader, R. F. W. *Inorg. Chem*. **1996**, *35*, 3954.

(28) Gillespie, R. J.; Robinson, E. A. *Angew. Chem., Int. Ed. Engl*. **1996**, *35*, 495.